

Effective Temperature Variations in IR Laser Induced Chemical Reactions. The Decomposition of Cyclobutanone

Vladimir Starov, Nur Selamoglu, and Colin Steel*

Chemistry Department, Brandeis University, Waltham, Massachusetts 02254 (Received: July 28, 1980)

A phenomenological model consistent with experimental studies of multichannel systems in the collisional regime is proposed. In particular the importance of "temperature" variation resultant from laser excitation with respect to the rationalization of the pressure dependence of both product yields and product ratios is discussed. An approach is outlined for estimating the "effective temperature" which influences the rate of collision-induced transitions. It is pointed out, with cyclobutanone as the main example, how the experimental results are quite dependent on the laser powers used and how careful absorption measurements are required before a system can be modeled in a meaningful fashion.

Introduction

Multichannel reactions, in which a single substrate has more than one reaction pathway,¹ as well as multisubstrate systems, in which more than one substrate undergoes reaction,² afford convenient probes for the infrared laser chemist interested in the nature of the excitation and the resulting energy distribution. The chemistry of multisubstrate systems has been employed to demonstrate the presence of "nonthermal" effects at low pressures and high fluences. In this paper, however, we shall be more concerned with multichannel reactions, and some of these have been gathered together in Table I. Their status is somewhat confused. In studying the decomposition of ethyl vinyl ether (EVE), Rosenfeld et al.^{1a} found no pressure dependence in the ratio of the products and indicated that their results were compatible with a thermalized system at a temperature of ~ 1600 K. The four-channel isomerization of vinylcyclopropane (VCP) was studied by Farneth et al.^{1c} They also found no pressure dependence in the product ratios but suggested that their results were compatible with a "nonthermal" model of the type suggested by Braun et al.^{2a} In contrast, in studying the decomposition of cyclobutanone (CB), Back and Back^{1e} and Harrison et al.^{1f} all observed significant pressure dependences in their product ratios. However, although the experiments were carried out under apparently similar conditions, Back and Back reported that the ratio ethene/(propene + cyclopropane) decreased with decreasing pressure while Harrison et al. observed exactly the opposite.

Because of our interest in CB^{1d} and because of the apparently contradicting data, we decided to reexamine the system to see whether we could rationalize the data in

terms of a reasonably quantitative model.

Experimental Section

A Lumonics TEA CO₂ laser tuned to either the R(12) line at 1073.3 cm⁻¹ or the P(20) line at 1046.9 cm⁻¹ was employed to irradiate samples in either a 10- or 25-cm stainless-steel cell (3.4-cm internal diameter) equipped with KCl windows. A 2:1 beam condenser fitted with ZnSe lenses was used for the collimated beam experiments, providing a beam of fluence up to 3.5 J/cm² and area 0.7 cm². A 5-in. focal length ZnSe lens was used in the focused-beam experiments to focus the beam at the center of the cell.

Energy measurements were performed by using a split beam. A calibrated Scientech Model 36-0001 disk calorimeter was used to measure transmitted fluences, the reference beam being monitored by a Lumonics 20D pyroelectric meter. The calorimeter output was integrated by a Spectra-Physics Autolab System I integrator.

The cyclobutanone (Aldrich Chemical Co.) was degassed immediately before use; it contained less than 1 part in 10⁵ of the expected products, ethylene, cyclopropane, and propylene. Irradiated and control samples were analyzed for the same compounds by FI gas chromatography using Porapak Q and Porapak T columns.

Results

Except where specifically stated, CB was irradiated at 1073.3 cm⁻¹. Energy-absorption measurements and chemical-decomposition data are summarized in Table II. Transmittance in terms of fluence was never less than 77% and typically was greater than 90%. Under these conditions the sample can be considered exposed to an average fluence, $\bar{F} = 1/2(F_0 + F_t)$, which is approximately constant along the cell path length. Although the absolute fluence measurements were rather precise, the determination of $\langle n \rangle$, the average number of photons absorbed per molecule, which depends upon the difference between F_0 and F_t , was significantly less so, as can be seen from the table.

In the collimated beam experiments (beam area 0.7 cm², first 16 entries) the products were only ethene (ET), cyclopropane (CP), and propene (PE), the latter coming from secondary isomerization of hot CP. Entries 1-14 refer to 1073.3 cm⁻¹ while 15 and 16 are for 1046.9 cm⁻¹. The data are presented in terms of $R = Y_1/Y_2 = [ET]/([CP] + [PE])$ where Y_1 and Y_2 are the yields from the lower and higher activation energy channels, respectively. The results for irradiation at 1073.3 cm⁻¹ are plotted as circles in Figure

(1) (a) Rosenfeld, R. N.; Brauman, J. I.; Barker, J. R.; Golden, D. M. *J. Am. Chem. Soc.* 1977, 99, 8063. (b) Brenner, D. M. *Chem. Phys. Lett.* 1978, 57, 357. (c) Farneth, W. E.; Thomsen, M. W.; Berg, M. A. *J. Am. Chem. Soc.* 1979, 101, 6468. (d) Steel, C.; Starov, V.; Leo, R.; John, P.; Harrison, R. G. *Chem. Phys. Lett.* 1979, 62, 121. (e) Back, M. H.; Back, R. A. *Can. J. Chem.* 1979, 57, 1511. (f) Harrison, R. G.; Hawkins, H. L.; Leo, R. M.; John, P. *Chem. Phys. Lett.* 1980, 70, 555. (g) Richardson, T. H.; Setser, D. W. *J. Phys. Chem.* 1977, 81, 2301. (h) Baklanov, A. V.; Molin, Yu. N.; Petrov, A. K. *Chem. Phys. Lett.* 1979, 68, 329. (i) Sudbo, Aa. S.; Schulz, P. A.; Grant, E. R.; Shen, Y. R.; Lee, Y. T. *J. Chem. Phys.* 1979, 70, 912.

(2) (a) Tsang, W.; Walker, J. A.; Braun, W.; Herron, J. T. *Chem. Phys. Lett.* 1978, 59, 487. (b) Danen, W. C.; Munslow, W. D.; Setser, D. W. *J. Am. Chem. Soc.* 1977, 99, 6961. (c) Gutman, D.; Braun, W.; Tsang, W. *J. Chem. Phys.* 1977, 67, 4291. (d) Danen, W. C. *J. Am. Chem. Soc.* 1979, 101, 1187. (e) Danen, W. C. *Opt. Eng.* 1980, 19, 21.

TABLE I: Multichannel Reactions Induced by Pulsed Infrared Lasers

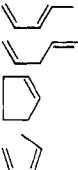
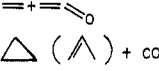
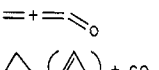
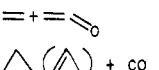
absorber	reactant	channels	pressure range, torr	fluence range, J/cm ²	energy absorbed, photon/molecule	ref
CH ₂ =CH-OC ₂ H ₅ (EVE)	EVE	CH ₃ CHO + C ₂ H ₄ CH ₂ CHO + C ₂ H ₅	5-440	focused		1a
EVE	EVE	CH ₃ CHO + C ₂ H ₄ CH ₂ CHO + C ₂ H ₅	0.002-15	0.5-0.9		1b
 (VCP)	VCP		0.2-1.1	5 ± 1, not collimated		1c
NH ₃	(CB)	 =+= 	50	0.3-0.8, collimated	1.5-2.8	1d
CB	CB	=+= 	0.6-10	<1, collimated	5.0 ± 0.3	1f
CB	CB	=+= 	0.2-9.8	~3, collimated and focused	see text	this work
C ₂ H ₄ FBr (BFE)	BFE	HBr + C ₂ H ₃ F HF + C ₂ H ₃ Br	0.6	3.1, not collimated		1g
C ₂ H ₄ FCl (CFE)	CFE	HCl + C ₂ H ₃ F HF + C ₂ H ₃ Cl	10 ⁻³ -5	focused		1h

TABLE II: Cyclobutanone Absorption and Decomposition Data

P, torr	L, cm	F ₀ , J/cm ²	F _t , J/cm ²	$\langle n \rangle$, photons/molecule	R	% decomp per pulse in irradi vol	no. of pulses
0.182	25.0				86 ± 15	0.80 ± 0.06	100
0.297	25.0	3.39 ± 0.03	3.36 ± 0.03	11 ± 5			
0.329	10.0	3.09 ± 0.09	3.05 ± 0.06	13 ± 19	79 ± 3	1.8 ± 0.1	100
0.425	10.0	3.13 ± 0.03	3.11 ± 0.16	8 ± 18	67 ± 4	2.5 ± 0.1	100
0.513	25.0	3.41 ± 0.03	3.33 ± 0.03	9 ± 3			
0.536	10.0	3.14 ± 0.10	3.12 ± 0.07	5 ± 17	62 ± 3	3.1 ± 0.2	100
0.802	10.0	3.52 ± 0.05	3.45 ± 0.04	13 ± 3	48 ± 3	7.9 ± 0.7	60
1.44	25.0	3.41 ± 0.02	3.15 ± 0.02	10.0 ± 0.7			
1.96	25.0				38 ± 3	19 ± 4	20
2.03	25.0	3.45 ± 0.04	3.06 ± 0.04	11.0 ± 0.5			
3.08	25.0	3.21 ± 0.02	2.58 ± 0.02	13.1 ± 0.4	38 ± 3	29 ± 3	10
5.47	10.0	3.40 ± 0.03	2.95 ± 0.03	12.0 ± 0.9	28 ± 3	48 ± 2	10
7.66	10.0	3.18 ± 0.06	2.60 ± 0.07	12.1 ± 0.8	28 ± 3	42 ± 1	10
9.84	10.0	3.47 ± 0.07	2.66 ± 0.06	12.5 ± 0.9	24 ± 5	23 ± 2	10
0.509	25.0	2.63 ± 0.02	2.59 ± 0.02	5 ± 3	61 ± 2	2.2 ± 0.1	100
5.18	25.0	2.61 ± 0.07	1.89 ± 0.03	8 ± 1	21 ± 1	20 ± 1	10
				F _{CH₄}			
0.49	10.0			0.0036	16 ± 1	44 ± 6	11
1.07	10.0			0.0061	18 ± 3	54 ± 1	5
2.49	10.0			0.0097	18 ± 3	81 ± 2	3
4.87	10.0			0.035	17 ± 1	135 ± 6	1
8.05	10.0			0.056	16 ± 2	310 ± 20	1
10.0	10.0			0.19	5 ± 1	510 ± 60	1

1. Best lines representing the data of Harrison et al. (solid) and Back and Back (dashed) are also shown.

Several focused-beam experiments were also carried out at 1073.3 cm⁻¹ (entries 17-22 and squares in Figure 1). Although no methane was detected in the collimated-beam experiments, it was found in the focused-beam experiments, and the column headed F_{CH₄} = [CH₄]/([ET] + [PE] + [CP]) gives the results. The fact that methane is formed and that its yield increases with pressure indicates the onset of secondary processes. Also at the two highest pressures, visible light emission from the sample was de-

tected. These two entries are therefore not plotted in Figure 1. In contrast to collimated-beam experiments in this and a previous study^{1d} where we could approach but never exceed 100% reaction per pulse in the irradiated area, in the focused-beam experiments at high pressures we exceeded 100% decomposition (see Table II). In this case the maximum irradiated volume was calculated from burn patterns at the cell windows and from the focal spot size. This suggests that reaction must "spread out" from the irradiated volume due to collisions with surrounding cold reactant.

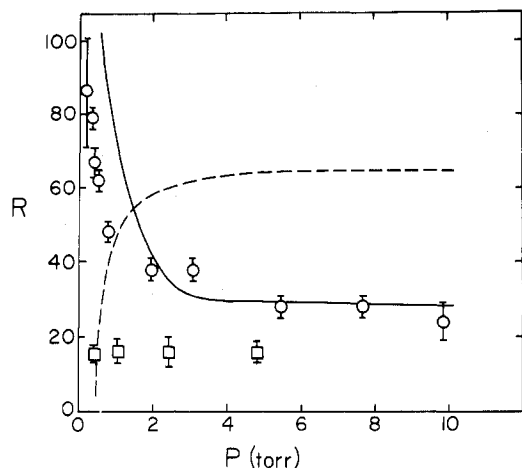


Figure 1. Experimental product ratios $R = \text{ethene}/(\text{cyclopropane} + \text{propene})$ as a function of cyclobutanone pressure for $\nu_{\text{tr}} = 1073.3 \text{ cm}^{-1}$: (O) this work, collimated beam $F_{\text{av}} \approx 3.2 \text{ J/cm}^2$; (□) this work, focused beam; (—) and (---) best lines through data of Harrison et al.^{1f} and Back and Back,^{1e} respectively.

Thermal Conversion Model

In the following we present a model which will quantify some of our arguments. It falls into the category of an energy-grained master equation (Appendix); however, there are several modifications to the usual approach.³ In particular we allow for effective "temperature" variation following laser excitation. Since this affects the magnitude of the collisional rate coefficients (see eq 6), it will be shown to have an important effect on product distributions and yields.

Because of the strongly nonequilibrium character of the laser-excited systems, the notion of "temperature" should be used rather carefully. However, we introduce a temperature-like parameter, T_{vib} , which monitors vibrational excitation due to interaction of molecular vibrations with the laser field. If at $t = 0$, $T_{\text{vib}} = T_0$ and if during a short subsequent time interval Δt an amount of energy ΔE_{vib} is deposited in the vibrations by the laser field

$$T'_{\text{vib}}(\Delta t) = T_0 + \Delta E_{\text{vib}}(\Delta t)/C_{\text{vib}}(T_0) \quad (1)$$

where $C_{\text{vib}}(T_0)$ is the vibrational heat capacity at T_0 . The vibrations are now "hotter" than the translational and rotational degrees. So by analogy with heat flow between bodies we write

$$\Delta T_{\text{rt}}/\Delta t = k_{\text{vrt}}P(T'_{\text{vib}} - T_{\text{rt}}) \quad (2)$$

where k_{vrt} ($\text{s}^{-1} \text{ torr}^{-1}$) is the rate constant for $V \rightarrow T/R$ energy flow and P (torr) is the pressure of the system. This results in V -cooling and T/R -heating so that finally at time Δt

$$T_{\text{vib}}(\Delta t) = T'_{\text{vib}}(\Delta t) - \Delta T_{\text{rt}}C_{\text{rt}}/C_{\text{vib}}(T_{\text{vib}}) \quad (3)$$

$$T_{\text{rt}}(\Delta t) = T_0 + \Delta T_{\text{rt}} \quad (4)$$

C_{rt} , the T/R heat capacity, is simply $3R$ for the temperatures under consideration. Using relations 1–4 and knowing the amount of energy absorbed by the system in any given time interval, $\Delta E_{\text{vib}}(\Delta t)$, one can compute the time variation in $T_{\text{vib}}(t)$ and $T_{\text{rt}}(t)$. Qualitatively, $T_{\text{vib}}(t)$ grows as long as laser energy is being absorbed while $T_{\text{rt}}(t)$ grows with a characteristic delay dictated by the value of

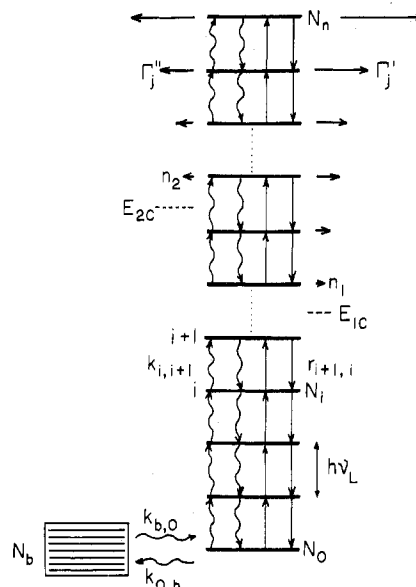


Figure 2. Schematic of the thermal conversion model. Terms are defined in the text.

k_{vrt} and the pressure of the system.

The model is shown schematically in Figure 2. The vibrational manifold is represented by a number of energy shells^{3e} positioned at energies $nh\nu_L$, $h\nu_L$ being the laser photon energy. The bottom vibrational level is connected by rotational relaxation processes $k_{b,0}$ and $k_{0,b}$ to the bath of rotational states associated with the ground vibrational level but which do not interact directly with the field. All energy shells are connected by radiative transitions (straight arrows) and by collisional processes (wavy arrows). The former are treated in the usual manner,^{3a} the rate coefficient for transition between levels i and $i + 1$ at time t being $r_{i,i+1} = I(t)\sigma_{i,i+1}$, where I ($\text{cm}^{-2} \text{ s}^{-1}$) and $\sigma_{i,i+1}$ (cm^2) are the laser intensity and the absorption cross section, respectively. The induced emission cross section is related to the latter via the densities of states at the levels i and $i + 1$, g_i and g_{i+1}

$$\sigma_{i+1,i} = \sigma_{i,i+1}g_i/g_{i+1} \quad (5)$$

assuming infinitely rapid redistribution of the oscillator strength between the degenerate states. $\sigma_{i,i+1}$ may vary with index i .

To treat the collisional part of the problem we make the following assumption. If an ensemble of oscillators with quantum energy ΔE is placed in a thermostat at temperature θ , when equilibrium is established the up and down collisional rate coefficients will be related through eq 6.

$$k_{i,i+1} = k_{i+1,i}(g_{i+1}/g_i)e^{-\Delta E/(R\theta)} \quad (6)$$

Although true equilibrium generally does not exist under laser excitation conditions, we identify θ with T_{rt} , the parameter monitoring rototranslational energy distribution. In fact θ is primarily expected to be influenced by T_{vib} . Since T_{rt} is never greater than T_{vib} , associating θ only with the former ensures that the role of thermal conversion is not overemphasized. Thus in our model absorption of laser radiation results in vibrational "heating" (eq 1) followed by partial thermalization (eq 2–4). This "thermal conversion" in turn affects the vibration transition rates (eq 6), which at high "temperatures" can compete favorably with radiative transitions. Because of this allowed "temperature" variation, vibrational Boltzmannization of the system occurs faster than in the case of a system in which the laddering constants are frozen at room tem-

(3) (a) Grant, E. R.; Schulz, P. A.; Sudbo, Aa. S.; Shen, Y. R.; Lee, Y. T. *Phys. Rev. Lett.* 1978, 40, 115. (b) Baldwin, A. C.; Barker, J. R.; Golden, D. M.; Dupperex, R.; van den Bergh, H. *Chem. Phys. Lett.* 1979, 62, 178. (c) Barker, J. R. *J. Chem. Phys.* 1980, 72, 3686 and references therein. (d) Lyman, J. L. *Ibid.* 1977, 67, 1868. (e) Stone, J.; Goodman, M. F. *Ibid.* 1979, 71, 408. (f) Stephenson, J. C.; King, D.; Goodman, M. F.; Stone, J. *Ibid.* 1979, 70, 4496.

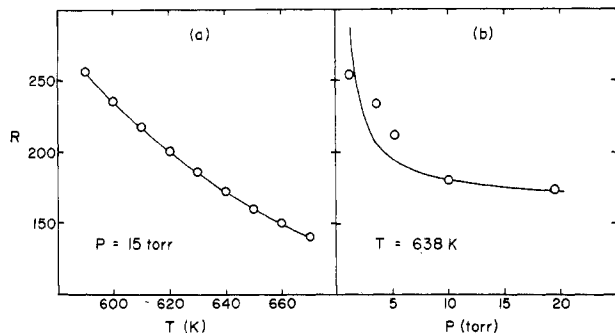


Figure 3. Variation in product ratio R for the thermal decomposition of cyclobutanone as (a) a function of temperature and (b) a function of pressure. Solid lines are model curves.

perature. As we shall see, this has a significant effect on the model predictions.

Discussion

Choice of Parameters. In order to fix some of the parameters associated with the nonradiative part of the model (see Appendix for details), we first fitted the pyrolysis data of Blades.⁴ Between 590 and 680 K he found $R = 1.6 \exp(3020/T)$. Points computed by using this equation together with the model fit are shown in Figure 3a. The calculations were performed with the laser field off ($I = 0$). It will be noted from the Appendix that we used a simple RRK-type expression as an empirical parametric formula to express the variation of the microscopic dissociation constants with energy. This approach is probably adequate especially when we are mainly interested in the ratio of rates. Full RRKM treatment requires estimating more than 27 parameters associated with each complex, and, given the present amount of data, it is doubtful whether such an approach would be any more fundamental or rigorous than the simple RRK approach which essentially uses thermal parameters together with an estimated value of s , the number of effective classical oscillators. In the Appendix we also discuss the choice of values for the collisional constants which range from a value of 2 MHz torr⁻¹ for $k_{1,0}$ to 40 MHz torr⁻¹ for $k_{n,n-1}$. The number of levels, $n + 1$, in the stepladder model was set at 35. This value is sufficiently large so that the uppermost levels are hardly populated during the computer experiment. Increasing n above this value therefore makes no difference to the results. Figure 3b shows the pressure dependence of R as predicted by the model in comparison with the experimental⁴ points. It can be seen that a very reasonable set of parameters affords a nice fit to both sets of data and that the only really arbitrary choice is the value of s .

The absorption data presented in Table II and Figure 4 allow estimates to be made of terms relevant to the radiative part of the model. Figure 4 shows that $\langle n \rangle$ levels off at ~ 12 photons/molecule for pressures higher than 2–3 torr. Owing to the uncertainty in the energy absorption at low pressures, we found it impossible to say whether $\langle n \rangle$ falls off at these pressures or remains constant as was suggested in ref 1f. We therefore calculated two model curves that approximate both possibilities (Figure 4). For

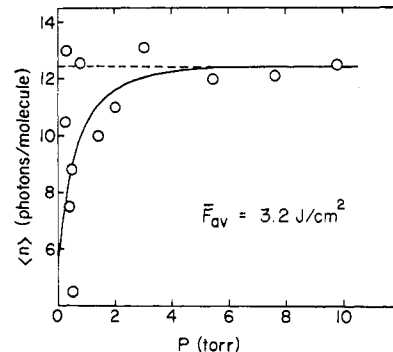


Figure 4. Variation in $\langle n \rangle$, the average number of photons absorbed per molecule, as a function of pressure for an average fluence $\approx 3.2 \text{ J/cm}^2$ and $\bar{\nu}_{\text{irr}} = 1073.3 \text{ cm}^{-1}$; (—) and (---) model curves for $f_0 = 0.3$ and 1.0, respectively. Other parameters defined in text.

the curve representing the case $\langle n \rangle = \text{a constant}$, we had to assume that molecules in all rotational states of the bottom pump level can interact with the field ($f_0 = 1$). For the curve exhibiting falloff the fraction of molecules interacting with the field, f_0 , was set to 0.3 and the rotational relaxation coefficient to the bath of levels, $k_{0,b}$, to 30 MHz torr⁻¹. The fractional value of $f_0 = 0.3$ is in fact in the range of those used by Stephenson et al. to explain their observations on the dissociation of CF_2HCl .^{3f} The value of $k_{0,b}$ is quite typical for rotational relaxation.¹⁰ Also from detailed balance $k_{b,0} = k_{0,b}f_0/(1 - f_0)$. The radiative interaction cross section was taken to be 10.2 ($f_0 = 1$) and $12.1 \times 10^{-20} \text{ cm}^2$ ($f_0 = 0.3$) and was independent of energy. The case of energy-dependent cross sections will be briefly discussed later. The model cross section $\sigma_{0,1}$ is related to the experimental one, σ_0 , via $\sigma_0 = f_0\sigma_{0,1}$ giving $\sigma_0 \approx 10 \times 10^{-20}$ and $4 \times 10^{-20} \text{ cm}^2$. These are in good agreement with the average cross section found experimentally, $\sigma_{\text{av}} = 1/LN_T \ln F_0/F_t$. From the data in Table II, $\sigma_{\text{av}} = (7 \pm 2) \times 10^{-20} \text{ cm}^2$.

Low-Fluence Regime. At this point we should like to stress that none of the parameters was further varied in the final calculations of R vs. P curves (Figure 5). These were carried out for reaction times, τ_r , 0.3 μs (= laser pulse time) and 1.0 μs . In the pressure range studied, the calculated ratio was in essence invariant with time after $\sim 1.0 \mu\text{s}$. Cooling of the reacting gas is expected to occur on the microsecond time scale at high pressures^{1d} and may take longer at low pressures. During cooling the instantaneous value of the ratio of the rates can vary rapidly. However, since the absolute yield will also be dropping off exponentially, the contribution to the overall ratio of yields should be small. This possibly explains why the model fits the observations so well despite its neglect of system evolution during cooling. In the low-fluence regime (3.2 J/cm^2) all of the calculated curves for $k_{\text{vrt}} > 0$ exhibit qualitatively similar pressure behavior closely resembling the data over the experimental pressure range. The cases in which k_{vrt} is set equal to zero and the high fluence data will be considered later.

Both in this work and in that of Harrison et al. 1073.3-cm⁻¹ radiation was employed while Back and Back used 1046.9 cm⁻¹.⁵ We therefore also carried out experiments at this frequency (entries 15 and 16 in Table II). If one compares these with entries 6 and 12, which were carried out at comparable pressures and fluences by using 1073.3-cm⁻¹ radiation, it can be seen that there appears to be no frequency specific effect and that we cannot

(4) Blades, A. T. *Can. J. Chem.* 1969, 47, 615.

(5) It was stated several times in ref 1e that P20 CO₂ laser line at 9.552 μm was employed in their studies, which contradicts another statement that all of the irradiations were carried out at 1059 cm⁻¹, made by the authors later in the text.

(6) Koren, G. *Appl. Phys.* 1980, 21, 65.

(7) Haarhoff, P. C. *Mol. Phys.* 1963–64, 7, 101.

(8) Frei, K.; Günthard, Hs. H. *J. Mol. Spectrosc.* 1960, 5, 218.

(9) Starov, V.; Steel, C.; Harrison, R. G. *J. Chem. Phys.* 1979, 71, 330.

(10) Townes, C. H.; Schawlow, A. L. "Microwave Spectroscopy"; McGraw-Hill: New York, 1955; p 351.

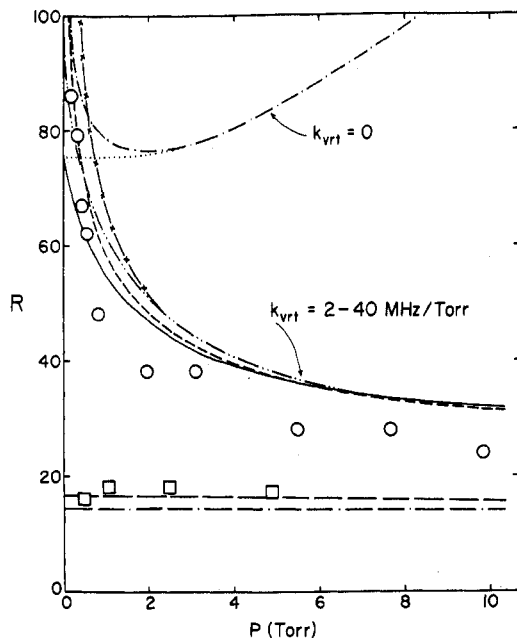


Figure 5. Comparison of model curves and experiment points for product ratio (R) as a function of pressure: (O) collimated beam, $F \approx 3.2 \text{ J/cm}^2$; (\square) focused beam, $F \approx 30\text{--}60 \text{ J/cm}^2$. Model curves are for the following:

	$\tau_r, \mu\text{s}$	f_0	$k_{vrt}, \text{MHz/torr}$	$F, \text{J/cm}^2$
(—)	0.3	1.0	2-40	3.2
(---)	1.0	1.0	2-40	3.2
(-·-)	1.0	0.3	2-40	3.2
(-x-) ^a	1.0	0.3	2-40	3.2
(···)	0.3	1.0	0	3.2
(-·-)	1.0	1.0	0	3.2
(-·-)	0.3 and 1.0	0.3 and 1.0	2-40 and 0	30
(-·-)	0.3 and 1.0	0.3 and 1.0	2-40 and 0	60

^a Energy-dependent cross section; see text and caption to Figure 6.

confirm the experimental findings of Back and Back.^{1e}

Importance of Thermal Conversion. Since experimentally we do not know the effective reaction times and since RRK treatments tend to systematically underestimate rate constants, we cannot predict absolute yields. Moreover, as indicated above, cooling dynamics can be quite complicated and are not included in the model. Figure 6 therefore shows yields for an arbitrary reaction time (1.0 μs), and attention should be paid to trends rather than the absolute values. The major point is that, in a system in which the collisional laddering constants are artificially maintained at "room temperature" (through $k_{vrt} = 0$ in this model), the yield decreases monotonically with pressure because of the dominance of down-laddering. On the other hand, if the effective temperature of the collisional constants increases ($k_{vrt} > 0$ in this model), the yield in general increases with pressure (---), at least over most of the pressure range. Notice, however, that for otherwise similar conditions curves for $k_{vrt} > 0$ and $k_{vrt} = 0$ tend to the same limit at $P = 0$, since radiative laddering dominates in this region. Calculations for reaction times $> 1 \mu\text{s}$ indicate that the yield continues to increase and that most decomposition may occur after the laser pulse is off, consistent with the calculations of Grant et al.^{3a}

The marked divergence between $k_{vrt} = 0$ and $k_{vrt} > 0$ is also apparent from the calculated product ratios (Figure 5). It can be seen that, in the low-fluence situation for $k_{vrt} = 0$, neither the general shape nor the actual values agree with the experimental data. Again the $k_{vrt} = 0$ and $k_{vrt} >$

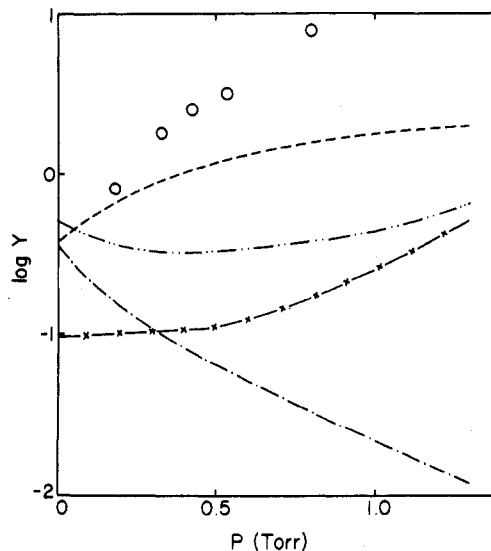


Figure 6. Percent decomposition per pulse (Y) in the irradiated volume as a function of pressure: (O) experimental data, collimated beam, $F \approx 3.2 \text{ J/cm}^2$. Model curves are for $F = 3.2 \text{ J/cm}^2$, $\tau_r = 1.0 \mu\text{s}$ and the following:

	$10^{19} \sigma_{0,11}, \text{cm}^2$	α	f_0	$k_{vrt}, \text{MHz/torr}$
(-·-)	1.02	0	1.0	2-40
(-·-)	1.21	0	0.3	2-40
(-x-)	1.50	-0.035	0.3	2-40
(-·-)	1.02	0	1.0	0

0 curves do coincide near $P = 0$. At higher pressures the $k_{vrt} > 0$ curve always lies below the corresponding $k_{vrt} = 0$ curve. This arises because collision-induced up conversion ($k_{i,i+1}$) is increased at higher "temperatures". This in turn favors the higher activation energy channel and so lowers R . In fact the upper curve (---) tends toward a value of $\sim 4 \times 10^4$, the ratio of the thermal rate constants at room temperature, while at 10 torr the lower curve (—) is already close to the value predicted by simply thermalizing the absorbed energy and carrying out decomposition at $\sim 940 \text{ K}$. Notice also the difference between curves having the same k_{vrt} and F but different τ_r values, e.g., (---) and (—). At $P = 0$ the higher R for the larger τ_r stems from the reaction which occurs after the laser field is off. Since in this domain there is no pumping to replenish upper levels and since the higher states are depleted most rapidly, the lower energy channel is favored, resulting in a larger value of R .

It is also of interest to notice (Figure 5) that, for laser fluence 60 J/cm^2 , the calculation for the case $k_{vrt} = 0$ practically coincides with that for $k_{vrt} > 0$. This is because at high fluences the radiative processes dominate collisional laddering, the average rate coefficient for the former being $2 \times 10^9 \text{ s}^{-1}$ and for the latter only $1 \times 10^8\text{--}3 \times 10^8 \text{ s}^{-1}$, even at 10 torr. This result also suggests that many "collisionless" models may correctly "predict" the experimental results obtained at high laser fluences, although they should fail when moderate energies sufficient to induce chemistry at higher pressures are employed.

High-Fluence Regime. In this region (fluence $30\text{--}60 \text{ J/cm}^2$) we compare the model calculations with the results obtained for the focused-beam decompositions. Although the laser fluence varies rapidly along the cell path length under these conditions, the major contribution to decomposition, and hence to the measured ratio, will come from the regions around the focal zone. Fluences as high as $\sim 60 \text{ J/cm}^2$ can be expected in the focal zone of a 5-in. lens⁶ when the fluence incident on the lens is $\sim 0.6 \text{ J/cm}^2$. We

therefore carried out calculations for $F = 30$ and 60 J/cm^2 . Very good agreement with the data can be seen for both curves. For these calculations the model predicts $\sim 100\%$ decomposition during the laser pulse time, 300 ns, at all pressures, and the curves for 1000 ns are not plotted since they would be indistinguishable from these calculated for 300 ns. Notice that the rapid variation in R with pressure is virtually absent at high fluences, a result consistent with the experimental findings of others in different systems studied under focused-beam conditions.^{1a,e,h} The model also predicts temperatures upward of $\sim 2000 \text{ K}$, clearly suggesting the spreading of the reaction out of the irradiated volume observed at higher pressures (see Table II).

Energy-Dependent Cross Sections. Several calculations were performed for the case of the radiative interaction cross section decreasing with energy, the rest of the parameters unchanged. To keep $\langle n \rangle$ at the experimentally observed value of 12.4 at high pressures, $\sigma_{0,1}$ was chosen slightly larger than for the case $\sigma_{0,1} = \sigma_{i,i+1} = \text{constant}$, $\sigma_{0,1} = 15.0 \times 10^{-20}$ and $12.8 \times 10^{-20} \text{ cm}^2$ for $f_0 = 0.3$ and 1.0 , respectively. α in eq 5A was chosen to be -0.035 ; i.e., the cross section drops to $1/2\sigma_{0,1}$ at level number 20. The computed curves agree quite well with respect to both shape and region of pressure dependence, and one of these is shown in Figure 5. The experimental data are not accurate enough to distinguish between the case $\alpha = 0$ and $\alpha < 0$. However, in the latter case the ratio increases with decreasing pressure a little more rapidly than in the former. This result is expected since, for lower cross sections at high energies, the retarded pumping rate should favor the lower activation energy channel, the effect being more pronounced at lower pressures where radiative interactions dominate the system behavior.

Comparison with the Decomposition Studies of EVE.^{1a} In addition to fitting our data, we decided to run some brief calculations to see whether we could explain the lack of pressure dependence of the product ratio for the decomposition of EVE in a focused beam. This was of interest because EVE has very different Arrhenius parameters for the decomposition channels as compared to CB, and the pressure range studied was also very different, 5–440 torr. Since the density of states function, as well as collisional relaxation rates, of EVE ($\text{C}_4\text{H}_8\text{O}$) are expected to be similar to those of CB ($\text{C}_4\text{H}_6\text{O}$), we simply set the parameters for the microscopic dissociation constants approximately equal to the experimental Arrhenius values for the EVE molecule; viz, $\lambda_1 = 1 \times 10^{11} \text{ s}^{-1}$, $E_1 = 190 \text{ kJ/mol}$, $\lambda_2 = 1 \times 10^{15} \text{ s}^{-1}$, $E_2 = 270 \text{ kJ/mol}$.

In addition we chose the number of effective oscillators to be $2/3$ of 33, the total number of oscillators in the EVE molecule, so $s_1 = s_2 = 22$. The rest of the model parameters were left unchanged. With a cross section $\sigma = 2 \times 10^{-20} \text{ cm}^2$ and for a fluence $F = 30 \text{ J/cm}^2$, our model predicts the ratios 0.40, 0.39, 0.39, 0.40, and 0.41 at 5, 15, 25, 233, and 440 torr, respectively. The experimental values found in ref 1a for the same pressure region are in the range of 0.39 ± 0.07 . Thus our calculations using very reasonable model parameters are in excellent agreement with the experimental findings of Rosenfeld et al.

Conclusions

It is shown how RRR parameters obtained from conventional thermal kinetic data in conjunction with cross sections derived from absorption measurements can be used to make estimates of most of the parameters required for the "thermal conversion" model proposed in this work. The model rationalizes the rather scanty experimental data currently available for infrared laser induced multichannel reactions in the collisional regime. Detailed modeling at

present is hampered especially by the paucity of energy-absorption measurements which should be a part of all experimental studies.

In the model attention is drawn to the important effect of "thermal conversion", i.e., effective "temperature" variation. This, through its effect on collisional up-pumping rates, affects both the absolute product yields and the product ratios especially in the low-intensity region characteristic of unfocused beams ($1\text{--}10 \text{ MW/cm}^2$). The effect is seen to be very large and should be taken into account in any model explicitly incorporating collisional relaxations.

We also show how the pressure dependence of the product ratio depends not only on unimolecular parameters related to molecular complexity and critical energies but also on the intensity of the radiation. Thus cyclobutanone shows pressure dependence of the product ratios when irradiated at intensities of $\sim 10 \text{ MW/cm}^2$ while no such dependence is observed at higher powers, $\sim 100 \text{ MW/cm}^2$. Such effects may explain why some authors have observed pressure dependence in product ratios while others have not even though the molecules may have been of comparable complexity and even had rather similar differences in their critical energies. In general the lack of pressure dependence in the product ratios is observed in focused-beam experiments, i.e., in the high-intensity regime. Furthermore, in this region, thermal conversion becomes less important since excitation is now dominated by radiative rather than collisional terms.

Acknowledgment. We thank Dr. R. G. Harrison for providing us a preprint of his article before publication. We also acknowledge generous financial support from Dow Chemical Corp. and from NIH through a Biomedical Support Grant to Brandeis University.

Appendix

The rate equations for the populations of the energy shells are

$$\begin{aligned} \dot{N}_i(t) = & (r_{i-1,i} + k_{i-1,i})N_{i-1}(t) + (r_{i+1,i} + k_{i+1,i})N_{i+1}(t) - (r_{i,i-1} + \\ & r_{i,i+1} + k_{i,i-1} + k_{i,i+1} + \Gamma_i' + \Gamma_i'')N_i(t) \quad i = 1, n-1 \\ \dot{N}_b(t) = & k_{0,b}N_0(t) - k_{b,0}N_b(t) \end{aligned}$$

$$\dot{N}_0(t) = k_{b,0}N_b(t) + (r_{1,0} + k_{1,0})N_1(t) - (r_{0,1} + k_{0,1} + k_{0,b})N_0(t)$$

$$\dot{N}_n(t) = (r_{n-1,n} + k_{n-1,n})N_{n-1}(t) - (r_{n,n-1} + k_{n,n-1} + \Gamma_n' + \Gamma_n'')N_n(t) \quad (1A)$$

$$N_b(0) = (1 - f_0)N_T$$

$$N_0(0) = f_0N_T$$

$$N_i(0) = 0 \quad i = 1, n$$

The number of photons absorbed per molecule by the time t , $n(t)$, is simply

$$n(t) = \frac{1}{N_T} \int_0^t \left[\sum_{i=1}^{n-1} (r_{i,i+1} - r_{i,i-1})N_i(t) + r_{0,1}N_0(t) - r_{n,n-1}N_n(t) \right] dt \quad (2A)$$

and the percentage yields of chemical channels $Y_1(t)$ and $Y_2(t)$ are

$$\begin{aligned} Y_1(t) = & \frac{100}{N_T} \int_0^t \left[\sum_{i=n_1}^n \Gamma_i' N_i(t) \right] dt \\ Y_2(t) = & \frac{100}{N_T} \int_0^t \left[\sum_{i=n_2}^n \Gamma_i'' N_i(t) \right] dt \end{aligned} \quad (3A)$$

Energy dependent dissociation rates were assumed of the form

$$\Gamma_i' = \lambda_1 \left(\frac{E_i - E_1}{E_i} \right)^{s_1} \quad \Gamma_i'' = \lambda_2 \left(\frac{E_i - E_2}{E_i} \right)^{s_2} \quad (4A)$$

with $E_i = ih\nu_L$, $\Gamma_i' = 0$ for $i < n_1$, and $\Gamma_i'' = 0$ for $i < n_2$. n_1 and n_2 are the indexes specifying the shells whose energies lie most closely above E_{1c} and E_{2c} , the experimental critical energies for decomposition from channels 1 and 2, respectively. Since CB has 27 vibrational modes, we used s_1 and $s_2 = 18$, i.e., the familiar prescription that the number of effective oscillators is $\sim 2/3$ the total number of oscillators. In the same spirit λ_1 , E_1 , λ_2 , and E_2 were chosen to be consistent with the experimental Arrhenius parameters, viz, $3.6 \times 10^{14} \text{ s}^{-1}$, 217 kJ mol^{-1} , $2.3 \times 10^{14} \text{ s}^{-1}$, and 242 kJ mol^{-1} .

The density of states at energy E_i , g_i , was calculated by using Haarhoff's formula⁷ for anharmonic oscillators in conjunction with the known vibrational frequencies of the CB molecule.⁸ g_i values were used to calculate $r_{i+1,i}$ and $k_{i+1,i}$ values from the corresponding upward rate coefficients through 5 and 6.

Provision was made in the model for variation in the radiative interaction cross section with energy by taking it to be of the form suggested by Grant et al. (eq 5A).^{3a}

$$\sigma_{i,i+1} = \sigma_{0,1} \exp(\alpha i) \quad (5A)$$

The time-dependent radiative pumping rate coefficients, $r_{i+1,i}(t)$ were evaluated for a temporal pulse envelope closely matching the experimentally observed shape,⁹ $I(t) = At \exp(-t/t_{\max})$, where $A = F[t_{\max}^2 - (\tau_P + t_{\max})t_{\max} \exp(-\tau_P/t_{\max})]^{-1}$ with $\tau_P = 300 \text{ ns}$, $t_{\max} = 40 \text{ ns}$, and F the overall fluence.

All collisional rate coefficients were expressed through gas-kinetic collision frequency $Z \approx PT_{\text{rt}}^{1/2}$ and a β number, the reciprocal of the number of collisions required for a particular relaxation event to occur, $k = Z\beta$. For a large polar molecule like CB, we estimated Z at room temperature at 30 MHz torr^{-1} . For rotational relaxation $\beta_{\text{rot}} \approx$

1 often holds¹⁰ and so we assumed $k_{0,b} = 30 \text{ MHz torr}^{-1}$. We were unable to find any vibrational relaxation data for this molecule, but deactivation of the lower levels can be estimated from Lambert-Salter plots¹¹ and relaxation data for similar molecules. The number used in our calculations was $k_{1,0} = 2 \text{ MHz torr}^{-1}$. At higher vibrational levels, relaxation is known to be more efficient,^{12a} the amount of energy transferred per collision often exceeding several kcal mol⁻¹.^{12b} We therefore set $k_{n,n-1}$ for the deactivation of the top level in our model ($\sim 100 \text{ kcal}$ above the ground state) to 40 MHz torr^{-1} . For deactivation of the intermediate levels we used linear interpolation:

$$k_{i+1,i} = k_{1,0} + (k_{n,n-1} - k_{1,0})i/n \quad (6A)$$

Finally, to evaluate k_{vrt} , the coupling between vibrational and rotational/translational degrees of freedom, we identified this coupling with the rate of vibrational deactivation. This is reasonable because, whenever a vibrational deactivation event occurs, the mismatch of vibrational energy will be accommodated by the rotations and/or translations. We can thus write eq 7A, where \bar{i} is the mean

$$k_{\text{vrt}} = k_{1,0} + (k_{n,n-1} - k_{1,0})\bar{i}(t)/n \quad (7A)$$

excitation level, $\bar{i}(t) = \sum_{i=0}^n i f_i(t)$, $f_i(t)$ being the fraction of molecules in level i at time t . But, since $\bar{i}(t)$ is increasing with $T_{\text{rt}}(t)$ and since the choice of the form of k_{vrt} (eq 7A) is rather arbitrary, to reduce the computational effort we substituted a function of $T_{\text{rt}}(t)$ in place of $\bar{i}(t)$:

$$k_{\text{vrt}} = k_{1,0} + (k_{n,n-1} - k_{1,0}) \frac{T_{\text{rt}}(t) - T_0}{5T_0} \quad (8a)$$

where T_0 is the initial temperature of the sample, usually 298 K . The above equation gives $k_{\text{vrt}} = k_{1,0}$ when $T_{\text{rt}} = T_0$, and $k_{\text{vrt}} = k_{n,n-1}$ when $T_{\text{rt}} = 6T_0 = 1788 \text{ K}$.

(11) Lambert, J. D. "Vibrational and Rotational Relaxations in Gases"; Clarendon Press: Oxford, England, 1977.

(12) (a) Stevens, B. "Collisional Activation in Gases"; Pergamon Press: Oxford, England, 1967. (b) Rabinovitch, B. S.; Carroll, H. F.; Rynbrandt, J. D.; Georgakakos, J. H.; Thrush, B. A.; Atkinson, R. *J. Phys. Chem.* 1971, 75, 3376.